

## Microchannel-type Air Detective Sensor using the Change of Dielectric Constant for Medical Applications

Joon-Hwan Shim\*, Kyung-Hwa Kim\*, Kyung-Rak Sohn\*, Seok-Je Cho\*\*, Eung-Soo Kim\*\*\*

\*(Department of Electronics and Communications Engineering, Korea Maritime University, Pusan, Republic of Korea)

\*\* (Division of IT Engineering, Korea Maritime University, Pusan, Republic of Korea)

\*\*\* (Division of Digital Information Engineering, Pusan University of Foreign Studies, Pusan, Republic of Korea)

### ABSTRACT

Air embolism can be a potentially fatal complication of surgical procedures when air or sub-atmospheric is introduced under pressure into a body cavity. For the diagnosis and the treatment of air embolism quickly and efficiently, we have developed the air detector using microstructure capacitive sensor. The sensor consists of micro-channel on Pyrex 7740 glass with upper and lower electrodes which function as a capacitor. For air sensing, we designed air detection system with air control equipment, capacitance-to-frequency (C-F) signal processing and conversion circuit and LabVIEW monitoring system. In experiments with the system, the proposed system showed a frequency difference depending on the amount of air in the micro-channel of the sensor.

**Keywords** – Air detector, Capacitive sensors, Micro-channel, Dielectric constant, LabVIEW

### I. INTRODUCTION

Air embolism is an uncommon, but potentially catastrophic, event that occurs as a consequence of the entry of air into the vasculature. Vascular air embolism is a potentially life-threatening event that is now encountered routinely in the operating room and other patient care areas. Small amount of air will usually gets absorbed but larger amount air could go into one of the organs and obstruct the blood vessel and cause permanent damage or even death. Venous air embolism occurs when air enters the systemic venous circulation and travels to the right ventricle and pulmonary circulation. In contrast, arterial air embolism occurs when air enters the arterial system. Arterial air embolism can produce ischemia in any organ that has insufficient collateral circulation [1][2][3][4].

Real-time monitoring of continuous heart sound in patients detected by precordial Doppler ultrasound is, thus, vital for early detection of venous air embolism (VAE) during surgery. A disadvantage of the Doppler method is that it requires the constant attention of the anaesthetist to detect subtle changes in the doppler heart sound (DHS). In addition, quantitative information on the volume of air entering circulation cannot be provided simply by listening to the audio DHS [5][6].

Recently one study on the air detector using relative dielectric constant was published. It suggested that the sensor could detect existence of air using dielectric constant change. The sensor was made by a tygon tube

with two electrodes which function as a capacitor [7]. Another study on capacitive air bubble detector for moving blood in artificial kidney was reported. It was to evaluate if capacitor device can detect the presence of air bubbles of different diameters when entered the capacitor area. The sensor was composed of two platinum plates for the capacitor [8].

The objective of this work was to develop a micro channel-type capacitive sensor using glass wet micromachining which has many advantages such as downsizing, lightweight, low cost, high performance, mass production. In this paper, we investigated the effect of air content in water using the principle of capacitance and demonstrated that smooth inner surfaces of micro-channels were achieved by using a wet chemical etching, and the depth of micro-channel could be precisely controlled by adjusting the etching time. The developed sensor consists of micro-channels on Pyrex 7740 glass with upper and lower electrodes which function as a capacitor. Sensor outputs were obtained by the capacitance-to-frequency (C-F) converter circuit which is highly sensitive and accurate. The existence and amount of air according to the frequency change was also real-time recorded by PC using LabVIEW monitoring program.

### II. EXPERIMENTAL

**2.1 Principle and structure of sensor:** The capacitance of parallel plates as shown in Fig. 1 is given by the expression (1) when  $A$  is the area of the parallel metallic plates and  $d$  is separation between the plates.

$$C = \epsilon_r \epsilon_o \frac{A}{d} \quad (1)$$

Where  $\epsilon_o$  is the dielectric constant of free space,  $\epsilon_r$  is the relative dielectric constant of isolator,  $A$  is area of the two plates and  $d$  is distance between the two plates.

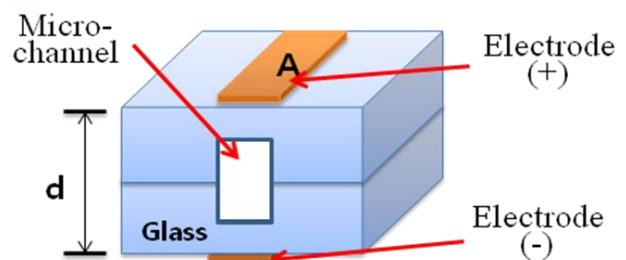


**Fig. 1.** The proposed sensor structure

In the parallel-plate capacitor geometry, it is expected that the capacitance will increase if a dielectric sample is inserted. This assumption is based on the parallel electric field lines used in capacitance calculation. Because of the large difference of the relative dielectric constant of air ( $\epsilon_r = 1$ ) and water ( $\epsilon_r = 80$ ), one of the most obvious methods for the detection of air-in-water is the measurement of the dielectric constant of the mixture. If the water mixture with small air volume flows in the micro-channel of the sensor, the dielectric constant of the mixture can be changed with the change of air volume. Then by the change of the dielectric constant, the capacitance of the micro-channel will be changed according to the air volume of the mixture.

**2.2 Fabrication process:** The detailed sequence for the fabrication of the sensor is shown in Fig. 2. The starting material was a Pyrex glass 7740 wafer of 500  $\mu\text{m}$  thickness. The Pyrex 7740 glass (Pyrex glass) is one of the most representative silicate-based materials that are widely used in many fields of MEMS/NEMS and it is used as a bond material with silicon, a mold for nanoimprint lithography and in medical devices, among other uses [9]. The fabrication process of the micro channel-type sensor is mainly divided by photolithography, lift-off, metal deposition, glass wet etching, glass to glass bonding, flow channel connection. Table 1 shows the detailed process condition. For the glass etching pattern, we used the lift-off process instead of metal etching process. After formation of the etching pattern, the glass was etched in the mixture solution with HF:  $\text{H}_3\text{PO}_4$ : DI water = 5: 70: 25 at 70°C for about 1 hour. In order to examine the surface state and etching depth of the etched glass, we used optical microscope and Tencor alpha-step surface profiler and

scanning electron microscope (SEM) imaging. The two etched glass wafer were then carefully aligned and pressed together to make a spontaneous bonding. The bonding process was achieved by annealing in a programmable furnace at 550°C for about 15 hours. The next step is the formation of electrode on the bonded glass wafer using Cu film with 50  $\mu\text{m}$  thickness. This step needs a photolithography adjustment from back to front side. Finally in order to obtain the fluid channel of inlet and outlet, the tygon tubes were attached to the etched channel of the glass wafer as shown in Fig. 3.

**Table 1.** Fabrication process condition

List of Figures	Process conditions
(a)	-Glass cutting: Sawing & placement equipment, 20 mm*20 mm -Glass cleaning: - RCA-1, RCA-2
(b)	-Photo Resist(PR) coating: Spin coater, AZ 5214
(c)	-UV-Exposure: Mask Aligner, 10 sec.
(d)	-PR develop: AZ 500, 30 min.
(e)	-Metal deposition: E-beam evaporator, Cr-100 nm/Au-50 nm
(f)	-Lift-off: Acetone solution in ultrasonic
(g)	-Glass etching: HF : $\text{H}_3\text{PO}_4$ : DI water = 5 : 70 : 25, 70°C, 1hr
(h)	-Metal remove: Cr/ Au etchant
(i)	-Glass to glass fusion bonding: 550°C, 15 hours
(j)	-Cu electrode formation: Cu film, 50 $\mu\text{m}$
(k)	-Flow channel connection: Tygon tube , inner diameter=0.7 mm , outer diameter=2.4 mm

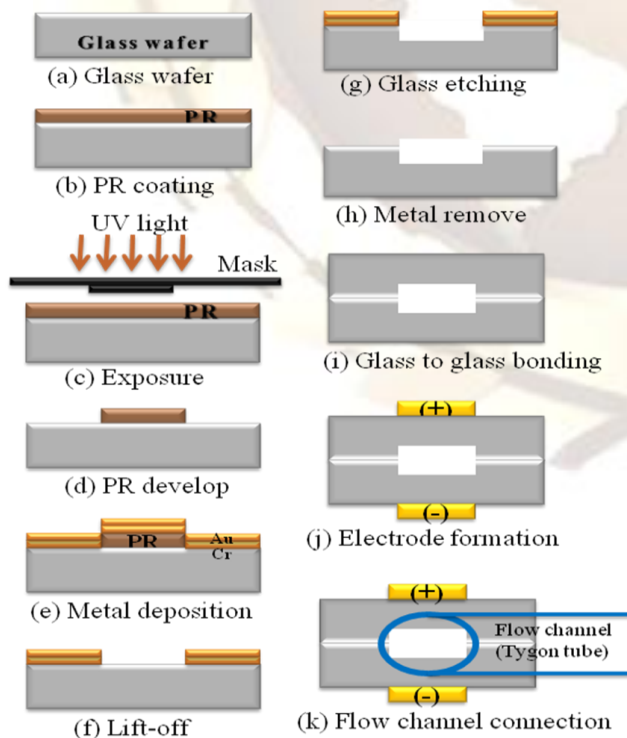


**Fig. 2.** Fabrication process sequence of the sensor

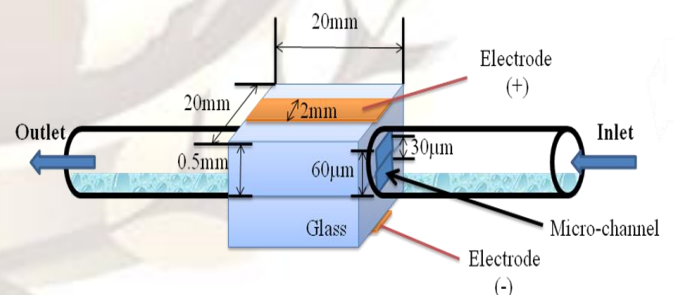


**Fig. 3.** The designed micro-channel sensor

**2.3 Measurement system:** The sensor can be divided into three principal parts as shown in the block diagram of Fig. 4: (1) the measurement head made by the electrodes along the fluid channel; (2) the capacitance-to-frequency converter; and the measurement data acquisition and (3) visualization system using DAQ board and LabVIEW program.

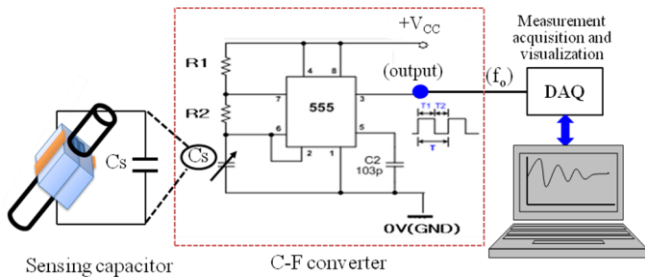


Fig. 4. Block diagram of the complete sensor system

The 555 timer produces a ‘square wave’. This is a digital waveform with sharp transitions between low (0V) and high (+V<sub>CC</sub>). The timer uses the sensor’s capacitance to create a square waveform [10]. A basis frequency is selected to correspond with the sensor’s capacitance at the given pure water. The C-F converter circuit can transfer the capacitance changes into the resonance frequency ( $f_o$ ) shifts by the expression (2).

$$f_o = \frac{1}{T} = \frac{1.44}{(R_1 + 2R_2)C_S} \quad (2)$$

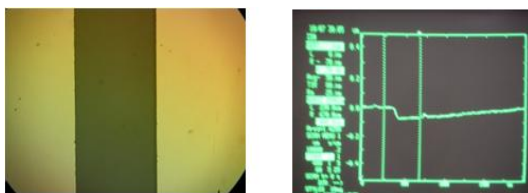
where

- $f_o$ : time period in seconds (Hz),
- T: time period in seconds (s),
- $R_1$ : resistance in ohms ( $\Omega$ ),
- $R_2$ : resistance in ohms ( $\Omega$ ),
- $C_S$ : capacitance in farads (F).

The capacitance variation due to the change of air content can lead to the output frequency change correspondingly. Simultaneously the output frequency  $f_o$  is then fed to the data acquisition and visualization system which is based on a 14-bit A/D data acquisition board, National Instruments PXI-6133, connected to a personal computer. A dedicated program written in LabVIEW allows the continuous visualization over time of the measured signals in order to estimate air content in water.

### III. RESULTS AND DISCUSSION

For fabrication of micro-channels on glass substrate, Au/Cr metal films were used as a wet chemical etch mask. The metal mask pattern was formed by lift-off process. The etching depth of the micro-channel can be well controlled by tuning the etching time. The remaining photo-resist was removed in acetone solution after wet etching. The etched channel pattern was observed by optical microscope and the etched depth was measured by alpha step. Fig. 5 shows optical images and alpha step profiles after lift-off and glass etching processes.



(a) Micro-channel image after lift-off process (metal thickness: 150 nm)



(b) Micro-channel image after etching time of 10 min.(etched depth: 4.97  $\mu\text{m}$ )



(c) Micro-channel image after etching time of 60 min.(etched depth: 29.82  $\mu\text{m}$ )

Fig. 5. Optical observation of the channels and alpha step profiles after lift-off and glass etching processes.

The thickness of metal mask film was 150 nm as shown in Fig. 5(a) which can provide a survival time of resist in wet etchant long enough to achieve up to 30  $\mu\text{m}$  thick channels. Fig. 5(b) and Fig. 5(C) are optical images after glass wet etching process. The etched depth after etching time of 10 minutes was about 4.97  $\mu\text{m}$  and the depth after etching time of 60 minutes was about 29.82  $\mu\text{m}$ . The observed etch rate is 0.5  $\mu\text{m min}^{-1}$ . We confirmed that the limit of etching time was 60 minutes because the edges and the boundary surface of the etched channel was damaged and the pinholes were observed on the metal surface. SEM imaging was performed to measure and confirm the thickness of micro-channels after the etching process. The cross-sectional SEM image of micro-channel after etching time of 60 minutes is shown in Fig. 6. The width of the micro-channel was 2 mm and the etched depth was 30  $\mu\text{m}$ . From this result, we can know that the result from alpha step and SEM image is the same. It can also be seen that the channels are of good uniformity and there is no significant deformation.

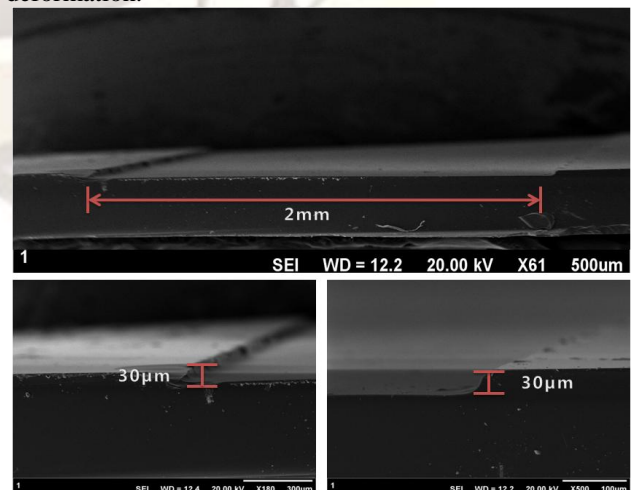
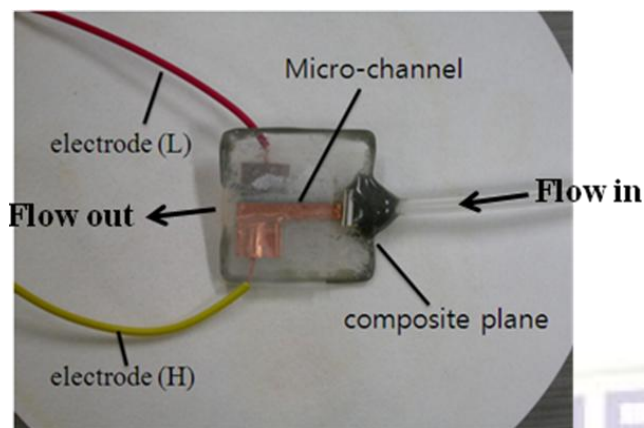
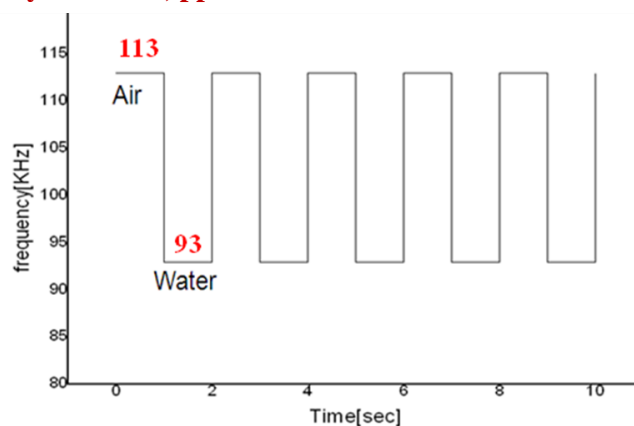


Fig. 6. Cross-sectional SEM image of micro-channel with depth of 30  $\mu\text{m}$  and width of 2 mm.



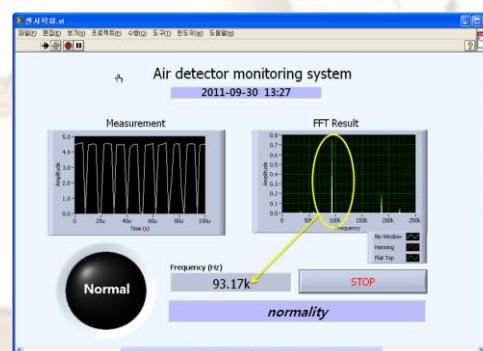
**Fig. 7.** The implemented prototype of micro-channel sensor

Fig. 7 shows the prototype of the sensor that was successfully used in sensing air. The sensor was made with the two etched glass wafer by glass to glass fusion bonding. The final height of the channel was  $60\ \mu\text{m}$  and the width was  $2\ \text{mm}$ . In order to make the fluid channel of inlet and outlet, the tygon tubes were attached to both sides of the etched channel of the sensor. We measured the capacitance variations in the two cases of only air and only water in the micro-channel. At the end of the tube channel, water or air are ejected into the micro-channel of the sensor. In the condition of channel completely filled with water or air, the sensor signals have been measured over an integration time of 5 seconds in no flow condition. The capacitances of the water or air were then determined at  $1\ \text{kHz}$  and room temperature using an external electrical probe and LCR meter. The measured capacitance of water content was  $21.9\ \text{pF}$  and the capacitance of air content was  $13.8\ \text{pF}$ . Thus the capacitance difference between water and air was about  $8\ \text{pF}$ . The sensor is connected in the C-F converter circuit which can transfer the capacitance changes into the resonance frequency. The reason why we use the converter circuit for sensor output is that the circuit is very sensitive to small capacitance changes. Fig. 8 shows that the output frequency is changed according to the existence of air. The measured frequency of water content was  $93\ \text{kHz}$  and the frequency of air content was  $113\ \text{kHz}$ . And the frequency difference was about  $20\ \text{kHz}$ . From this result, we can know that the difference of output frequency shows the existence of air in water. Thus we could decide that the developed sensor can apply for medical application such as the detection of air in blood because human blood has the same dielectric constant as water.

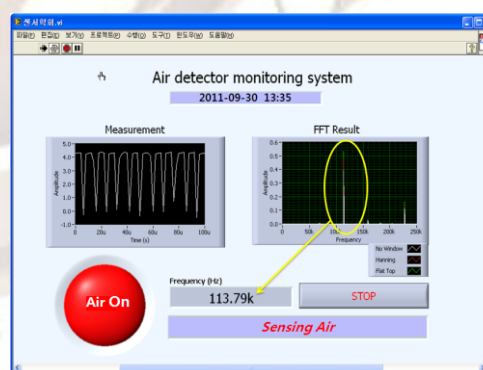


**Fig. 8.** Measured output frequency according to water and air contents

Fig. 9 shows the result of LabVIEW monitoring system. The LabVIEW system allows the continuous visualization over time of the measured values, the output frequency by FFT, the associated inrush of air. Fig. 9(a) shows the monitoring result in the cases of only water. Fig. 9(b) shows the monitoring result in the cases of only air. As air in water is detected by the sensor, the real-time monitoring system shows the warning message.



(a) water detection in micro-channel



(b) air detection in micro-channel

**Fig. 9.** Real-time LabVIEW monitoring system

#### IV. CONCLUSION

In this paper, we presented the applicability of a micro-channel capacitive sensor for the monitoring of air in blood. The introduction of air between the two plates of the capacitor with the micro-channel changes the capacitance which can be easily detected. In order to

detect the presence of air content in the micro-channel, we investigated the variations of frequency generated by the C-F converter. The capacitance sensor is connected in the converter circuit and delivered the capacitance of the sensor to the converter input. The variations of the capacitance of the sensor caused by the changes of two media with air and water causes a shift in the resonance frequency. The converter circuit is very sensitive to small capacitance changes, and the frequency shifts can be easily determined by continuous monitoring of LabVIEW system. The characteristics of the sensor showed acceptable frequency changes. The developed sensor can be used for medical application such as the detection of air in blood. This system has some merits compared to expensive ultrasonic equipment. It can also be made by simple structure and low cost. And the system could be applied in various fields where fluid flow problems occur by air existence.

#### ACKNOWLEDGEMENTS

This work was supported by the College of Engineering at Korea Maritime University.

#### REFERENCES

- [1] T.M. Dudney, and C.G. Elliott, Pulmonary embolism from amniotic fluid, fat, and air, *Progress in Cardiovascular Diseases*, 36(6), 1994, 447-474.
- [2] M.B. King, and K.R. Harmon, Unusual forms of pulmonary embolism, *Clinics in Chest Medicine*, 15(3), 1994, 561-580.
- [3] C.M. Muth, and E.S. Shank, Gas embolism, *New England Journal of Medicine*, 342(7), 2000, 476-482.
- [4] P.G. Jorens, E. Van Marck, A. Snoeckx, and P.M. Parizel, Nonthrombotic pulmonary embolism, *European Respiratory Journal*, 34(2), 2009, 452-474.
- [5] B.C.B. Chan, F.H.Y. Chan, F.K. Lam, P.W. Lui, and P.W.F. Poon, Fast detection of venous air embolism in Doppler heart sound using the wavelet transform, *IEEE Transactions on Biomedical Engineering*, 44(4), 1997, 237-246.
- [6] M.A. Mirski, A.V. Lele, L. Fitzsimmons, and T.J.K. Toung, Diagnosis and treatment of vascular air embolism, *Anesthesiology*, 106(1), 2007, 164-177.
- [7] H.S. Lee, and C.W. Kim, A study on the air detector using relative dielectric constant, *Journal of the Sensor Science and Technology*, 16(5), 2007, 384-388.
- [8] M.G. Abdalrahman, A.B. Adam, and J.O. Dennis, Capacitive air bubble detector for moving blood in artificial kidney, *The 3<sup>rd</sup> International Symposium. On Biomedical Engineering*, Bangkok, Thailand, 2008, 332-337.
- [9] S.W. Youn, and C.G. Kang, Maskless pattern fabrication on Pyrex 7740 glass surface by using nano-scratch with HF wet etching, *Scripta Materialia*, 52(2), 2005, 117-122.
- [10] D.G. Cinthiya, and R. Jegan, A novel seat occupancy detection system based on capacitive sensing for airbag control, *ICETT*, 2011, 1-3.